Regional differences in cell characteristics in electric eel electric organs indicate electrocyte development with ventral to dorsal migration.

Sinlapachai Senarat [1, 2], Ayako Matsumoto [3], Shintaro Sakaki [2], Daichi Tsuzuki [2], Kazuko Uchida [4], Makoto Kuwahara [4], Eiichi Hondo [2, 3] and Atsuo Iida [2, 3, *]

[1] Division of Biological Science, Faculty of Science, Prince of Songkla University, Kho Hong, Hat Yai District, Songkhla 90110, Thailand

[2] Department of Animal Sciences, Graduate School of Bioagricultural Sciences, Nagoya University, Furo-cho, Chikusa-ku, Nagoya, 464-8601, Japan

[3] Department of Animal Sciences, School of Agriculture, Nagoya University, Furo-cho, Chikusa-ku, Nagoya, 464-8601, Japan

[4] Institute of Materials and Systems for Sustainability, Nagoya University, Furo-cho, Chikusa-ku, Nagoya, 464-8601, Japan

***Correspondence:** Atsuo Iida

Email: tol2.4682@gmail.com

Keywords: cell differentiation, electrocytes, Electrophorus, Na^+/K^+-ATPase

Abstract

Electric eels (*Electrophorus*) are renowned for their ability to generate electric discharge, which is used for prey capture and defense. Their electric organs (EOs) are located along the lateral–ventral region of the tail and contain electrocytes, which are multinucleated syncytium cells. Two major hypotheses for the electrocyte origin are proposed: (1) muscle fibers or their precursors, and (2) mesodermal cells not via muscle lineage. In this study, we demonstrate the likely molecular mechanisms and processes involved in this differentiation, supporting the second hypothesis. We report the regional differences in cell morphology within the main EO (mEO) of *Electrophorus*. The cell morphology and distribution from the ventral terminal to the dorsal region of the mEO suggest the segregation of progenitors from the ventral cluster and their gradual transformation into mature multinucleated electrocytes via the layering and proliferation stages along the dorsal axis. Myosin-positive muscle cells were not included in the mEO differentiation process. Immunohistochemistry revealed strong expression of sodium-potassium adenosine triphosphatase (Na^+/K^+-ATPase), a key component in generating electric discharge in the mEO, across most mEO regions, except in the ventral cluster cells. Based on these observations, we propose that electrocyte progenitors develop from ventral cluster cells in the mEO and differentiate into mature multinucleated cells as they migrate dorsally. This is the first report to approach the developmental process of *Electrophorus* electrocytes from cell morphology and genetic profiles. Our findings represent a breakthrough in understanding the differentiation of electrocytes during the growth stages of *Electrophorus*.

Introduction

Electric fish include multiple classified species, such as electric rays, catfish, and eels. As Charles Darwin described in his work *On the Origin of Species* (Chapter 6: Difficulties on Theory), “The electric organs of fishes offer another case of special difficulty; for it is impossible to conceive by what steps these wondrous organs have been produced” (Darwin, 1859). Darwin's question of how these electric species appeared independently in each taxon is difficult and remains elusive. Here, we address this question from the perspective of cell and molecular biology using electric eels (*Electrophorus*).

The electric eel, an electric fish, was originally described by Carl Linnaeus in 1766 as *Gymnotus electricus* and was later revised as *Electrophorus electricus* by Theodore Gill in 1864 (Jordan, 1963). Recently, they have been reclassified into three distinct species, *E. electricus*, *Electrophorus varii*, and *Electrophorus voltai*, based on both morphological and genetic sequence data (de Santana et al., 2019). Electric eels are known for their ability to generate electric discharges, with a maximum capacity of 860 V for *E. voltai* (de Santana et al., 2019). They possess three types of electric organs (EOs): the main electric organ (mEO), Hunter’s organ, and Sachs’ organ, which are located in the lateral-ventral region of the tail (Williamson, 1775; Hunter, 1775; Sachs, 1877). The mEO is the largest among the three. It appears as early as the juvenile stage (total length [TL], 15 mm) (Schwassmann et al., 2014), but the other two appear at later stages, around a TL of 23 cm (Moller, 1995). The mEO is predicted to play a role in high-voltage discharge for prey capture or defense, whereas the other organs are considered to play a role in low-voltage discharge for sensing and communication (Xu et al., 2021). The cells responsible for electric discharge in an EO are multinucleated syncytia called electrocytes (Luft, 1957). Early studies suggested that electrocytes are derived from muscle lineage precursors (Fritsch, 1883). Recent histological observations of the mEO in juvenile *Electrophorus* suggest that the EO consists of electrocytes budded from a specified cell cluster named the electromatrix, located in the ventral region of the skeletal muscle (Schwassmann et al., 2014). More detailed observations and multifaceted analyses of *Electrophorus* embryos are required to determine the distinct origin and developmental mechanisms of the first electrocytes. However, artificial breeding methods have not yet been established; therefore, obtaining embryos in the laboratory is challenging. As an alternative model, a weakly electric fish, *Brachyhypopomus gauderio*, a species related to *Electrophorus* belonging to the same order

(*Gymnotiformes*), was used to observe developmental stages, including EOs, under laboratory conditions (Alshami et al., 2020). In this species, cell clusters consisting of Pax7^{+}/Myosin^{-} cells in the ventral region of the myotome were reported as the EO primordium. Based on these studies, the developmental origin of electrocytes in electric species of *Gymnotiformes* is considered to be the ventral cell cluster derived from somite lineage cells rather than from differentiated myocytes. In these studies, electrocyte lineage cells were classified into two populations: mature electrocytes and immature cells located in the ventral cluster. However, suppose one or both stages consist of multiple "substages." In this case, their clarification is expected to lead to a more detailed description of the differentiation process of electrocyte lineage cells. Moreover, researchers have focused on the developmental origin of electrocytes; however, the source of these cells during growth remains elusive.

From another perspective, advances in molecular biology methods have enabled the comparison of gene expression between EOs and other tissues, including skeletal muscle. In EOs, some muscle characteristic genes were downregulated, whereas other genes not expressed in the muscle were upregulated (Gallant et al., 2014; Gallant, 2019). Specifically, genes for ion transporters or channels, such as *atp1a*, *chrna*, *scn4aa*, and *kcnj12*, are upregulated not only in electric eels, but also in other electric fish species (Thompson et al., 2018; LaPotin et al., 2022). Some functional mutations were found in the genes encoding the ion transporters of *Electrophorus* compared to non-electric species. Substitutions in the amino acid sequences of these proteins have been predicted to contribute to high-voltage discharge in electrocytes (Traeger et al., 2017), and this modification is considered crucial for high-voltage electric discharge in *Electrophorus* spp. The molecular genetic characteristics of mature electrocytes are well known; however, how these expressed genes affect the differentiation of electrocytes remains unknown. Here, we report the progenitors of electrocytes based on histological observations and immunohistochemistry. Understanding the spatiotemporal distribution of ion transporter proteins in the EO is essential for understanding electrocyte differentiation.

Methods

Animal experiments

This study was approved by the Ethics Review Board for Animal Experiments at Nagoya University (approval number: A240105-002). All experiments involving live animals were conducted in strict accordance with institutional guidelines to ensure humane treatment. Electric eels used in this study were purchased from Meito Suien Co., Ltd. (Nagakute, Japan). The specimens used for histology were too young (TL: 10–15 cm) to determine their distinct species and sex; thus, we treated them as *Electrophorus sp*. (*Electrophorus*) in this study. The specimen used for sequencing analysis was a female with a developed ovary and was presumed to be *E. electricus* based on genome information.

Histology and histochemistry

The electric eels were euthanized using a rapid cooling shock to ensure that they were unresponsive to gill movements and external stimuli (Wilson et al., 2009). Tail region cross-sections (5 mm thick) were dissected and fixed in 4% paraformaldehyde solution for 24 h at room temperature for histological observations. Fixed samples were then dehydrated in a graded ethanol series, cleared in xylene, embedded in paraplast, and sectioned at 4 μm thickness using a Leica microtome (Leica, Germany) (Kongthong et al., 2023; Presnell and Schreibman, 2013; Suvarna et al., 2013). Three consecutive sections were stained with Harris' hematoxylin and eosin (HE) to observe body organization and tissue structure. Masson's trichrome (MT) staining was used to assess muscular structure and collagen fibers. Tissue samples were examined, photographed using an Olympus BX53 microscope, and imaged using a DP25 digital camera (Olympus, Shinjuku, Japan) or a BZ-X800 microscope (Keyence, Osaka, Japan).

Electron microscopy

The tail region of *Electrophorus* was sliced into 5 mm transverse sections and fixed in 2.5% glutaraldehyde, followed by washing with PBS. The fixed specimens were treated with 1% osmium tetroxide in PBS for 60 min and dehydrated in a graded ethanol series (50%, 70%, 80%, 90%, 95%, 99.5%, and 100%). Samples were treated with propylene oxide (KISHIDA CHEMICAL, Osaka, Japan) and embedded in epoxy resin (Nissin EM Quetol-812). The blocks

were polymerized at 60°C for 48 h. Sections of 1 μm thickness were stained with toluidine blue and observed using a Nikon ECLIPSE LV100ND with a DP74 digital camera (Olympus) to determine the region of interest. Sections of 100 nm thickness were cut using a Leica ultramicrotome and stained with UranyLess (Micro to Nano) and 3% lead citrate (Micro to Nano). Backscattered electron images were obtained using an SU9000 field-emission scanning electron microscope (Hitachi, Tokyo, Japan) at 1 kV.

RNA sequencing

Total RNA was extracted from the mEO and skeletal muscle of an adult female electric eel using an RNeasy Plus Mini kit (QIAGEN). Next-generation sequencing (NGS) was performed by Macrogen Japan Corp. (Tokyo, Japan) using a NovaSeq6000 platform (Illumina, Inc., San Diego, CA, USA). Approximately 40 million 100 bp paired-end reads were obtained for each sample. NGS data were deposited in the DNA Data Bank of Japan (DDBJ; ID: PRJDB17973).

Transcriptomic analysis

The calculation of differentially expressed genes was performed using the National Institute of Genetics' supercomputer at the Research Organization of Information and Systems. The adaptor and noise sequences were removed using the fastp program version 0.23.2 (https://github.com/OpenGene/fastp) (Chen et al., 2018). The cleaned reads were mapped to the genome of *Electrophorus electricus* (GCA_003665695.2, https://asia.ensembl.org/*Electrophorus*_electricus/Info/Index/) using the HISAT2 program version 2.2.1 (https://daehwankimlab.github.io/hisat2/) (Kim et al., 2019). The number of mapped reads was calculated using the featureCounts program in the subread package version 2.0.6 (https://subread.sourceforge.net/) (Liao et al., 2013, 2014). Further calculations were performed using the R software on a personal computer. Differentially expressed genes were identified using the edgeR package version 3.42.4 (https://bioconductor.org/packages/release/bioc/html/edgeR.html) with the following thresholds: false discovery rate < 0.05, and fold change > 2.00 (Robinson et al., 2010). A volcano plot was generated using the enhanced volcano package version 1.20.0 (https://github.com/kevinblighe/EnhancedVolcano).

Immunohistochemistry

Consecutive sections from the histological protocol were prepared on slides coated with glycerol-albumin (Mayer's fixative). The slides were deparaffinized in xylene, hydrated through a decreasing ethanol series, washed in tap water, and treated with 0.5% Triton X-100/PBS for 30 min and 0.3% H_2O_2 for 10 min to inactivate endogenous peroxidase activity. The sections were blocked with Blocking One solution for 2 h at room temperature (03953-95, Nacalai Tesque, Kyoto, Japan). The sections were incubated overnight at 4°C with either anti-NKA α1 (a5-s, DSHB, IA, USA, 1:5 in Blocking-One solution) or myosin heavy chain (F59-s, DSHB, 1:5 in Blocking-One solution) hybridoma supernatants. This was followed by incubation with Horse Anti-Mouse IgG Antibody (H+L) Peroxidase (PI-2000, Vector Laboratories, Inc., Burlingame, CA, USA, 1:500 dilution in 0.1% Tween-20/PBS) for 2 h at 4°C. Staining was performed by incubation with 3,3'-diaminobenzidine tetrahydrochloride (SK-4105, Vector Laboratories, Inc.) for 5 min at room temperature. Finally, the slides were dehydrated and mounted using Permount (SP15-100, Thermo Fisher Scientific). A control section without primary antibody was prepared to ensure the specificity of staining. Sodium-potassium adenosine triphosphatase (Na^+/K^+-ATPase [NKA]) localization was examined and photographed using the same method used for histological observations.

Results

Morphological observations of electrocytes

Electrophorus has its mEO in the tail region, which is the largest of the three organs responsible for electric discharge. In this study, especially in the histological analysis, the specimens were regarded as too young to observe well-developed Hunter's and Sach's organs; thus, they were excluded from the analysis. The mEO is located ventral to the skeletal muscle and consists of multinucleated syncytia called electrocytes (Figure 1A, 1B). The electrocytes were layered along the dorsal–ventral and anterior–posterior axes (Figure 1B). The series of cells along the anterior–posterior axis increases the membrane potential and generates a high-voltage discharge. Cell morphology along the dorsal–ventral axis is critical for understanding how electrocytes develop in the body; thus, we examined the histological morphology of electrocytes using MT staining (Figure 1C). In the dorsal region of the mEO, we observed the typical structure of mature multinucleated electrocytes placed in a non-cellular compartment with an extracellular space around the cell body, which is important for generating a membrane potential for discharge. In the ventral region, such distinct extracellular spaces were not observed, and square cell bodies without protrusions filled the compartment (Figure 1D). This morphological difference was also confirmed by the observation of toluidine blue-stained ultrathin sections and electron microscopy. Electron microscopy indicated that ventral electrocyte nuclei exhibited various shapes compared with those in the dorsal region. The presence and morphology of the mitochondria and caveolae showed no distinct differences between cells in the dorsal and ventral regions (Figure 1E). Through these experiments, we identified electrocytes with a previously unreported morphology in the ventral region of the mEO.

Ventral terminal cell cluster in EO

The cell morphology of the mEO differed between the dorsal and ventral regions. Thus, a detailed examination of the cell morphology from the ventral to the dorsal terminus of the mEO was performed using HE and MT staining (Figure 2A). A characteristic cell cluster consisting of high-density nuclei was identified at the ventral terminus of the mEO. This cluster was separated from the adjacent muscle layer by collagen fibers. In contrast, a structural border was not observed between the cluster and the dorsal region of the mEO (Figure 2B). The anti-

myosin signal, which labels myogenic cells, was not detected in ventral cluster cells (Figure 2C). This indicates that the cluster belonged to the mEO, but not the muscle layer. We then categorized the mEO into seven populations based on cell and tissue morphology (Figure 2D). The terminal cluster consisted of high-density mononuclear cells located in the ventral terminus of the mEO, and segregated cell clusters were observed in the dorsal position of the terminal cluster. Layers consisting of mononuclear cells appeared near the dorsal region. Proliferating cells in these layers and multinucleated electrocytes without extracellular space (immature electrocytes) were observed deep in the dorsal region. Mature electrocytes with extracellular spaces were observed over a broad area of the mEO. Finally, the mature mEO appeared to shrink near the dorsal skeletal muscles (Figure 2E). Thus, the morphology of the cells in the mEO changed drastically along the dorsal–ventral axis.

Gene expression in EO

Tissue fragments from the mEO and skeletal muscles were excised via macroscopic surgery, and total RNA was extracted from each tissue. The RNA samples were subjected to NGS, and the resulting sequence reads were processed to determine gene expression values and visualize differences in gene expression between tissues (Figure 3A, Table S1, S2). Our analysis revealed higher expression levels of typical muscle functional factors, such as genes for actin, creatine kinase, myosin, and troponin, in the muscle compared to the mEO. Conversely, *N-myc downstream-regulated gene-4* (*ndrg4*) was found to be more highly expressed in the mEO (Table S3). The present study focused specifically on the membrane molecules responsible for generating membrane potential through ion transport, such as acetylcholine receptors and sodium/potassium transporters, which exhibit higher expression levels in the mEO than in skeletal muscle (Figure 3B, Table S3). Notably, genes encoding NKA subunits (*atp1a2a* and *atp1b2b*) were highly expressed in the mEO, based on RNA sequencing. Cation transporters are believed to be localized in the anterior part of electrocytes (Figure 3C). In the tail region of *Electrophorus*, the electrocytes align along the anterior-posterior axis of the trunk, which is responsible for generating a high-voltage current due to synchronous activation regulated by motor neurons (Figure 3D).

NKA distribution in EO

To evaluate electrocyte function, the presence and distribution of NKA protein in the mEO were detected using immunohistochemistry. The anti-NKA supernatant exhibited specific signals in the mEO and other organs, including the skeletal muscle and central nervous system, in *Electrophorus* (Figure 3E). In the electrocytes, the plasma membrane of the mEO was labeled with the supernatant. The sagittal section indicated the accumulation of NKA protein in the anterior part of the plasma membrane (Figure 3F). Additionally, the signals were lower in the ventral region of the mEO and absent in the ventral terminal cluster, even after longer chromogenic reactions (Figure 3G, 3H). NKA expression was detected in the initial layer stages in the mEO, but the signals did not exhibit membrane localization, which was observed during proliferation. Subsequently, strong membrane NKA signals were observed in immature and mature mEO tissues. An NKA signal was also detected in the shrunken tissue (Figure 3H). These data indicate that NKA is absent in the terminal cluster cells of the mEO but is upregulated and membrane-localized in the dorsal population cells, including mature electrocytes.

Discussion

We analyzed the generation of electrocytes in *Electrophorus* using histology and immunohistochemistry. Our analysis indicated that ventral cluster cells are promising electrocyte progenitor candidates in the mEO. We propose that these progenitor cells differentiate into electrocytes and migrate from the ventral to the dorsal region. NKA expression is absent in the ventral cluster, initiating from the monocellular stages and maintaining its expression in developed multicellular electrocytes. This is the first report to provide consecutive observations of EO development, indicating the origin of electrocytes in the post-embryonic stages of *Electrophorus*. Early studies alleged that EOs in electric fish were derived from muscle fibers or muscle lineage cells, based on morphological observations. Histological observations of electric rays and larval mormyrid fish suggest that their electrocytes differentiate from mature muscle fibers (Fox and Richardson, 1978; Srivastava and Szabo, 1972). In *Electrophorus*, electrocytes were considered to differentiate from muscle based on light microscopy observations (Fritsch, 1883; Szabo, 1966). These studies concluded that the presumed electrocyte progenitors exhibited striated muscle-like structures. In our study, such muscular structures were not found in the ventral region of the mEO, and the ventral muscle layer was separated from the mEO by collagen fibers. Furthermore, the mEO lacked myosin-positive cells, which are characteristic of muscle tissue. Therefore, our results do not support the hypothesis that the electrocytes of *Electrophorus* are derived from muscle lineage cells.

Other groups have claimed that electrocytes do not originate from differentiated muscle lineage cells, but are directly developed from mesodermal cells before cell fate commitment (Keynes 1961). Histological observations have identified cell clusters ventral to the myotome as potential precursors of electrocytes in *Electrophorus* and related species, such as the weakly electric *Brachyhypopomus gauderio* (Schwassmann et al., 2014; Alshami et al., 2020). However, they classified the candidate cluster and the developed EO as independent tissues in different locations, leaving no clear evidence to suggest a relationship between them. They used *Electrophorus* embryos obtained from the field because experimental breeding methods for handling embryos in laboratories had not yet been established. This problem still exists and does not allow the use of embryos in our experiment. Therefore, in the present study, juvenile fish prior to sexual maturation were used.

We identified a ventral terminal cell cluster in the mEO and observed continuous changes in cell morphology. Based on these data, we propose that the electrocytes originate as mononuclear progenitor cells in the ventral terminal cluster of the mEO and differentiate into multinucleated syncytia with dorsal migration (Figure 4). Although this study was limited by breeding methodology challenges in obtaining embryos under laboratory conditions and did not focus on embryonic stages, our findings on the source and differentiation of electrocytes during growth are crucial for understanding the molecular mechanisms underlying EO formation in *Electrophorus*.

We focused on sodium potassium adenosine triphosphatase (Na^+/K^+-ATPase, NKA) as a functional molecule involved in generating membrane potential in electrocytes. We observed that the transcripts per million values for the NKA subunits in the mEO were over 100-fold higher than those in the skeletal muscle. A previous study identified novel phosphorylation sites in the NKA protein of electric eels that were predicted to contribute to the high-voltage discharge of EOs (Traeger et al., 2017). NKA is ubiquitously distributed in animal tissues and plays an important role in generating membrane potential for cellular functions beyond those of electrocytes (Suhail, 2010). NKA is a popular sodium pump distributed not only in EOs but also in various types of cells; thus, anti-NKA signals were detected not only in the mEO but also in the skeletal muscle, kidney, brain, and other organs of *Electrophorus*. Notably, the ventral region of the mEO lacked anti-NKA signals, suggesting that ventral cluster cells are immature and unable to generate membrane potentials via the NKA ion pump. Cells in the ventral terminal cluster exhibit characteristic morphologies, such as small size, minimal cytoplasm, and round shape, which are typical characteristics of quiescent stem cells, including hematopoietic stem cells (HSCs) and muscle satellite cells (MuSCs) (de Morree & Rando, 2023; Pinho & Frenette, 2019; Siegel et al., 2011). Therefore, we propose that the ventral terminal cluster includes stem cells that differentiate into electrocytes. Furthermore, single-cell RNA sequencing or cell characteristic evaluation using stem cell markers contributes to a deeper understanding of the maintenance of terminal cluster cells and their differentiation into electrocytes. Methodological investigations using *Electrophorus* should be improved in future research.

Our finding that multinucleated cells in the dorsal region of the mEO more closely resemble the typical morphology of functional electrocytes than those in the ventral region supports the conventional theory that the ventral region includes electrocyte progenitors (Gotter et al., 1998).

Electrocytes in the dorsal terminus of the mEO shrank, and the tissue structure appeared to be disrupted. Therefore, we propose that the EO develops from stem cells in the ventral region, progresses to maturity with dorsal migration, and eventually regresses in the dorsal terminal. This 'Ventral-to-Dorsal' model does not conflict with previous reports (Szabo, 1966; Schwassmann et al., 2014). Our study enhances the understanding of the developmental process of EOs in *Electrophorus*. Further analyses using cutting-edge technologies, including NGS, are required to understand the molecular mechanisms by which EOs are generated in *Electrophorus*. A recent study proposed that changes in sodium channel expression are important for the evolutionary acquisition of EOs in weakly electric species (LaPotin et al., 2022). Darwin's question arose from the independent acquisition of EOs in several fish lineages. The present study provides detailed information on the origin and developmental process of EOs in the electric eel *Electrophorus*. Future application of our methods to other electric fish may ultimately lead to a solution to Darwin's question.

Acknowledgments

We acknowledge the fellowship granted to S.S. by the Matsumae International Foundation (Grant Number: MIF-23G04). This work was supported by the Japan Science and Technology Agency (JST), the Japan Society for the Promotion of Science KAKENHI (Grant Number: 21H04637 to M.K.), and the "Advanced Research Infrastructure for Materials and Nanotechnology in Japan (ARIM)" program of the Ministry of Education, Culture, Sports, Science, and Technology (MEXT) (Grant Number: JPMXP1223NU0016 to A.I.). Computations were partially performed on the supercomputer of the National Institute of Genetics (NIG) at the Research Organization of Information and Systems (ROIS). Yutaka Hattori arranged complimentary rentals of the digital microscope. Akihiko Koga and Akira Kanamori provided us with helpful comments. We are grateful for the constructive discussions with members of Unique-Kai, an annual meeting for biologists investigating non-conventional experimental animals in Japan.

References

1. Alshami, I. J. J., Ono, Y., Correia, A., Hacker, C., Lange, A., Scholpp, S., Kawasaki, M., Ingham, P. W., & Kudoh, T. (2020). Development of the electric organ in embryos and larvae of the knifefish, Brachyhypopomus gauderio. Developmental biology, 466(1-2), 99–108. https://doi.org/10.1016/j.ydbio.2020.06.010
2. Chen S, Zhou Y, Chen Y, Gu J. fastp: an ultra-fast all-in-one FASTQ preprocessor. Bioinformatics. 2018;34(17):i884-i890. doi:10.1093/bioinformatics/bty560
3. Darwin, C. & Kebler, L. (1859) On the origin of species by means of natural selection, or, The preservation of favoured races in the struggle for life. London: J.
4. de Morree, A., & Rando, T. A. (2023). Regulation of adult stem cell quiescence and its functions in the maintenance of tissue integrity. Nature reviews. Molecular cell biology, 24(5), 334–354. https://doi.org/10.1038/s41580-022-00568-6
5. de Santana, C. D., Crampton, W. G. R., Dillman, C. B., Frederico, R. G., Sabaj, M. H., Covain, R., Ready, J., Zuanon, J., de Oliveira, R. R., Mendes-Júnior, R. N., Bastos, D. A., Teixeira, T. F., Mol, J., Ohara, W., Castro, N. C. E., Peixoto, L. A., Nagamachi, C., Sousa, L., Montag, L. F. A., Ribeiro, F., Waddell, J. C., Piorsky, N. M., Vari, R. P., Wosiacki, W. B. (2019). Unexpected species diversity in electric eels with a description of the strongest living bioelectricity generator. Nature communications, 10(1), 4000. https://doi.org/10.1038/s41467-019-11690-z
6. Fox, G. Q., & Richardson, G. P. (1978). The developmental morphology of Torpedo marmorata: electric organ--myogenic phase. The Journal of comparative neurology, 179(3), 677–697. https://doi.org/10.1002/cne.901790313
7. Fritsch G (1883) Die elektrischen Fische im Lichte der Deszendenzlehre. In: Virchow R, von Holtzendorff FR (eds) Sammlung gemeinverständlicher wissenschaftlicher Vorträge, vol 835–898. Habel, Berlin
8. Gallant, J. R., Traeger, L. L., Volkening, J. D., Moffett, H., Chen, P. H., Novina, C. D., Phillips, G. N., Jr, Anand, R., Wells, G. B., Pinch, M., Güth, R., Unguez, G. A., Albert, J. S., Zakon, H. H., Samanta, M. P., & Sussman, M. R. (2014). Nonhuman genetics. Genomic basis for the convergent evolution of electric organs. Science (New York, N.Y.), 344(6191), 1522–1525. https://doi.org/10.1126/science.1254432
9. Gallant, J.R. (2019). The Evolution and Development of Electric Organs. In: Carlson, B.,

Sisneros, J., Popper, A., Fay, R. (eds) Electroreception: Fundamental Insights from Comparative Approaches. Springer Handbook of Auditory Research, vol 70. Springer, Cham. https://doi.org/10.1007/978-3-030-29105-1_4

10. Gotter, A. L., Kaetzel, M. A., & Dedman, J. R. (1998). *Electrophorus* electricus as a model system for the study of membrane excitability. Comparative biochemistry and physiology. Part A, Molecular & integrative physiology, 119(1), 225–241. https://doi.org/10.1016/s1095-6433(97)00414-5
11. Hunter, J. (1775). "An account of the Gymnotus electricus". Philosophical Transactions of the Royal Society of London (65): 395–407.
12. Jordan DS. 1963. The genera of fishes and a classification of fishes. Stanford: Stanford University Press, 330.
13. Keynes RD (1961) The development of the electric organ in *Electrophorus* electricus L. In: Chagas C, Paes de Carvalho A (eds) Bioelectrogenesis. Elsevier, Amsterdam, pp 14–19
14. Kim, D., Paggi, J. M., Park, C., Bennett, C., & Salzberg, S. L. (2019). Graph-based genome alignment and genotyping with HISAT2 and HISAT-genotype. Nature biotechnology, 37(8), 907–915. https://doi.org/10.1038/s41587-019-0201-4
15. Kongthong, K., Charoenphon, N., Thaochan, N., Boonyoung, P., Iida, A., Jeamah, A., Imsonpang, S, Wongkamhaeng,K., Kongtheng, P. & Senarat, S. (2023). A histological method for marine invertebrates. Vertinary Intergrative Science 21:251-163.
16. LaPotin, S., Swartz, M. E., Luecke, D. M., Constantinou, S. J., Gallant, J. R., Eberhart, J. K., & Zakon, H. H. (2022). Divergent cis-regulatory evolution underlies the convergent loss of sodium channel expression in electric fish. Science advances, 8(22), eabm2970. https://doi.org/10.1126/sciadv.abm2970
17. Liao, Y., Smyth, G. K., & Shi, W. (2013). The Subread aligner: fast, accurate and scalable read mapping by seed-and-vote. Nucleic acids research, 41(10), e108. https://doi.org/10.1093/nar/gkt214
18. Liao, Y., Smyth, G. K., & Shi, W. (2014). featureCounts: an efficient general purpose program for assigning sequence reads to genomic features. Bioinformatics (Oxford, England), 30(7), 923–930. https://doi.org/10.1093/bioinformatics/btt656
19. Luft, J. H. (1957). The histology and cytology of the electric organs of electric eel (*Electrophorus electricus L.*). Journal of Morphology, 100 (1), 113-139.

20. Moller, P. (1995) Electric fishes: history and behavior. Chapman & Hall, London
21. Pinho, S., & Frenette, P. S. (2019). Haematopoietic stem cell activity and interactions with the niche. Nature reviews. Molecular cell biology, 20(5), 303–320. https://doi.org/10.1038/s41580-019-0103-9
22. Presnell, J.K., & Schreibman, M. P. (1997). Humason's animal tissue techniques, 5th ed. US, Johns Hopkins University Press.
23. Robinson, M. D., McCarthy, D. J., & Smyth, G. K. (2010). edgeR: a Bioconductor package for differential expression analysis of digital gene expression data. Bioinformatics (Oxford, England), 26(1), 139–140. https://doi.org/10.1093/bioinformatics/btp616
24. Sachs, C. (1877). Beobachtungen und versuche am südamerikanischen zitteraale (*Gymnotus electricus*). Archives of Anatomy and Physiology, 66–95.
25. Schwassmann, H. O., Assunção, M. I., & Kirschbaum, F. (2014). Ontogeny of the electric organs in the electric eel, *Electrophorus* electricus: physiological, histological, and fine structural investigations. Brain, behavior and evolution, 84(4), 288–302. https://doi.org/10.1159/000367884
26. Siegel, A. L., Kuhlmann, P. K., & Cornelison, D. D. (2011). Muscle satellite cell proliferation and association: new insights from myofiber time-lapse imaging. Skeletal muscle, 1(1), 7. https://doi.org/10.1186/2044-5040-1-7
27. Srivastava, C. B., & Szabo, T. (1972). Development of electric organs of Gymnarchus niloticus (fam. Gymnarchidae). I. Origin and histogenesis of electroplates. Journal of morphology, 138(3), 375–385. https://doi.org/10.1002/jmor.1051380305
28. Suhail M. (2010). Na, K-ATPase: Ubiquitous Multifunctional Transmembrane Protein and its Relevance to Various Pathophysiological Conditions. Journal of clinical medicine research, 2(1), 1–17. https://doi.org/10.4021/jocmr2010.02.263w
29. Suvarna, K.S., Layton, C., Bancroft, J.D. (2013). Bancroft's theory and practice of histological techniques. 7th ed. Canada, Elsevier.
30. Szabo T. (1966). The origin of electric organs of *Electrophorus* electricus. The Anatomical record, 155(1), 103–110. https://doi.org/10.1002/ar.1091550112
31. Thompson, A., Infield, D. T., Smith, A. R., Smith, G. T., Ahern, C. A., & Zakon, H. H. (2018). Rapid evolution of a voltage-gated sodium channel gene in a lineage of electric fish leads to a persistent sodium current. PLoS biology, 16(3), e2004892.

https://doi.org/10.1371/journal.pbio.2004892

32. Traeger, L. L., Sabat, G., Barrett-Wilt, G. A., Wells, G. B., & Sussman, M. R. (2017). A tail of two voltages: Proteomic comparison of the three electric organs of the electric eel. Science advances, 3(7), e1700523. https://doi.org/10.1126/sciadv.1700523
33. Williamson, H. (1775). "Experiments and observations on the Gymnotus electricus, or electric eel". Philosophical Transactions of the Royal Society of London (65): 94–101.
34. Wilson, J.M., Bunte, R.M., & Carty, A.J. (2009). Evaluation of rapid cooling and tricaine methanesulfonate (MS 222) as methods of euthanasia in zebrafish (*Danio rerio*). Journal of the American Association for Laboratory Animal Science (48): 785–789.
35. Xu, J., Cui, X., & Zhang, H. (2021). The third form electric organ discharge of electric eels. Scientific reports, 11(1), 6193. https://doi.org/10.1038/s41598-021-85715-3

Figures

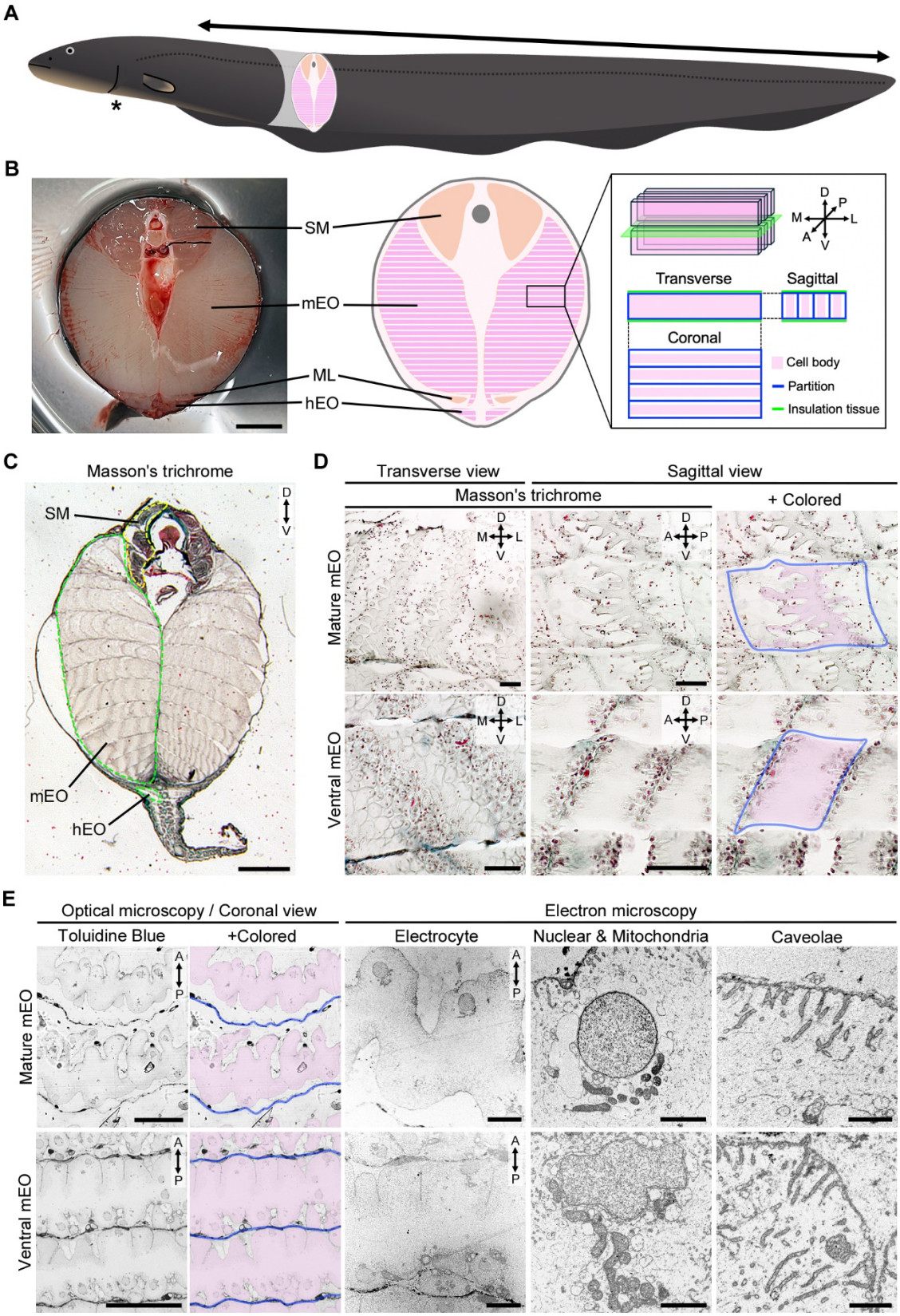
A
*
B
SM
mEO
ML
hEO
D
P
M
L
A
V
Transverse
Sagittal
Coronal
Cell body
Partition
Insulation tissue
C
Masson's trichrome
SM
mEO
hEO
D
V
D
Transverse view
Sagittal view
Masson's trichrome
+ Colored
Mature mEO
Ventral mEO
E
Optical microscopy / Coronal view
Electron microscopy
Toluidine Blue
+Colored
Electrocyte
Nuclear & Mitochondria
Caveolae
Mature mEO
Ventral mEO
A
P

Figure 1. Morphological differences of multinucleated electrocytes

A. Illustration of the whole body of *Electrophorus*. The double-headed arrow corresponds to the tail region of the body. The asterisk indicates the anus. **B**. A photograph and illustration of the transverse section of the tail region of *Electrophorus*. The medial–lateral lines in the mEO indicate the outer edge of the multinucleated electrocytes. The plate-shaped electrocytes are stacked along the anterior–posterior and dorsal–ventral axes. SM, skeletal muscle. mEO, main electric organ. Scale bar, 1 cm. **C**. A whole transverse section of the tail region, including the electric organ. Scale bar, 1 mm. **D**. Cell morphologies of the electrocytes in the dorsal and ventral regions of the mEO. The blue lines indicate the outer edges of the electric unit. The cell bodies of electrocytes (colored magenta) are within the unit. Scale bars, 50 μm. **E**. Ultrathin sections (100 nm) of the electrocytes observed by optical or electron microscopy. The blue lines indicate the outer edges of the electric unit. The cell bodies of electrocytes (colored magenta) are within the unit. Scale bars, 50 μm (toluidine blue), 10 μm (electrocyte), 2 μm (nucleus & mitochondria), 1 μm (caveolae). A, anterior; D, dorsal; M, medial; L, lateral; P, posterior; V, ventral; hEO, Hunter's electric organ; mEO, main electric organ; SM, skeletal muscle.

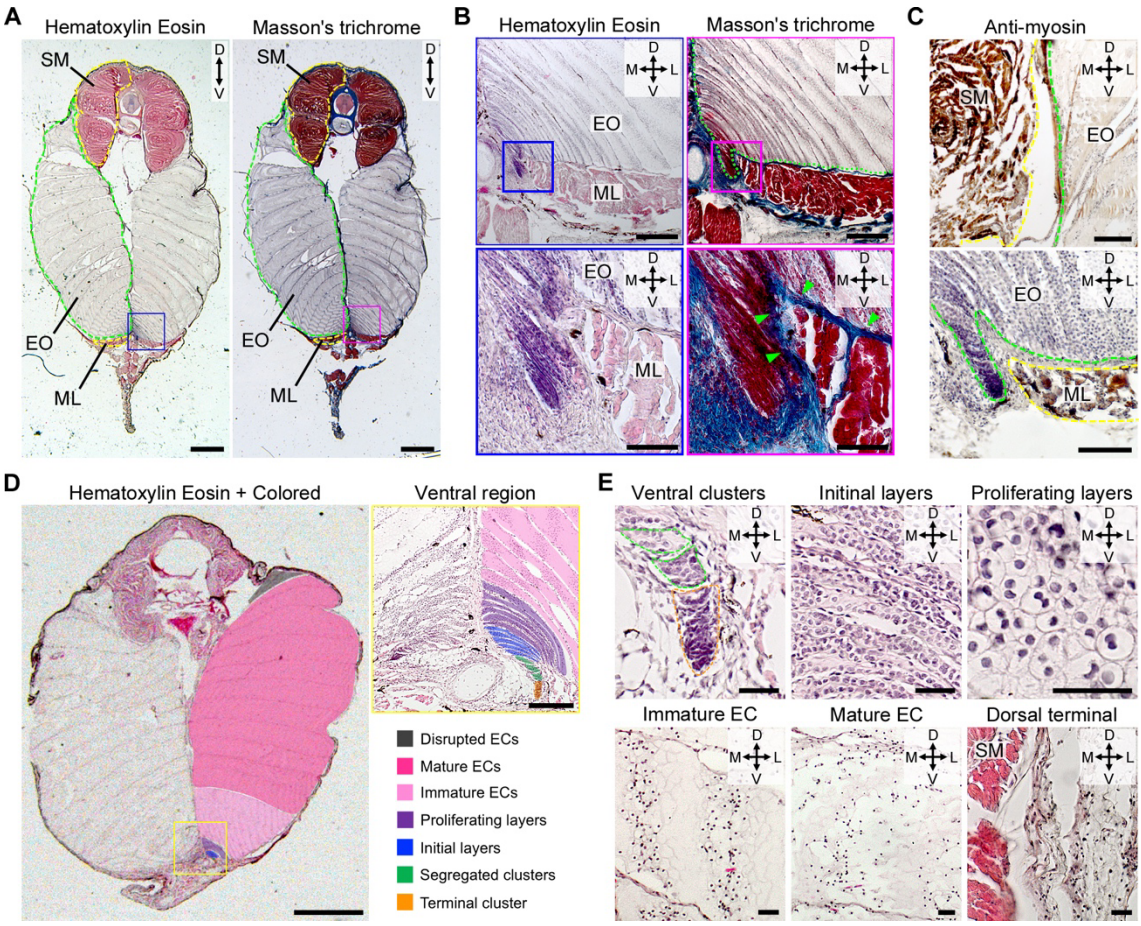

Figure 2. Morphological differences of cells along the dorsal–ventral axis

A. A whole transverse section of the tail region, including the electric organ. The green dotted line indicates the outer edge of the mEO. The yellow dotted lines indicate the outer edge of the muscular tissues. Scale bar, 1 mm. **B**. The ventral region of the mEO and the enlarged images of the ventral terminal cluster. The green dotted line indicates the outer edge of the mEO. The green arrowheads indicate the collagen fibers stained by Aniline Blue. Scale bars, 200 μm (low magnification), 50 μm (enlarged). **C**. Immunohistochemistry against myosin heavy chain in the dorsal and ventral positions. The muscular tissues show positive signals, but not in the mEO tissues. Scale bars, 100 μm (dorsal), 50 μm (ventral).

D. A whole transverse section colored roughly by cell morphology. Scale bars, 1 mm (whole section), 100 μm (enlarged). **E**. Enlarged images of each cell type in the mEO. The orange dotted line indicates the terminal ventral cluster. The green dotted lines indicate the segregated cell clusters. Scale bar, 20 μm. D, dorsal; M, medial; L, lateral; V, ventral; mEO, main electric organ; ML, muscle layer; SM, skeletal muscle.

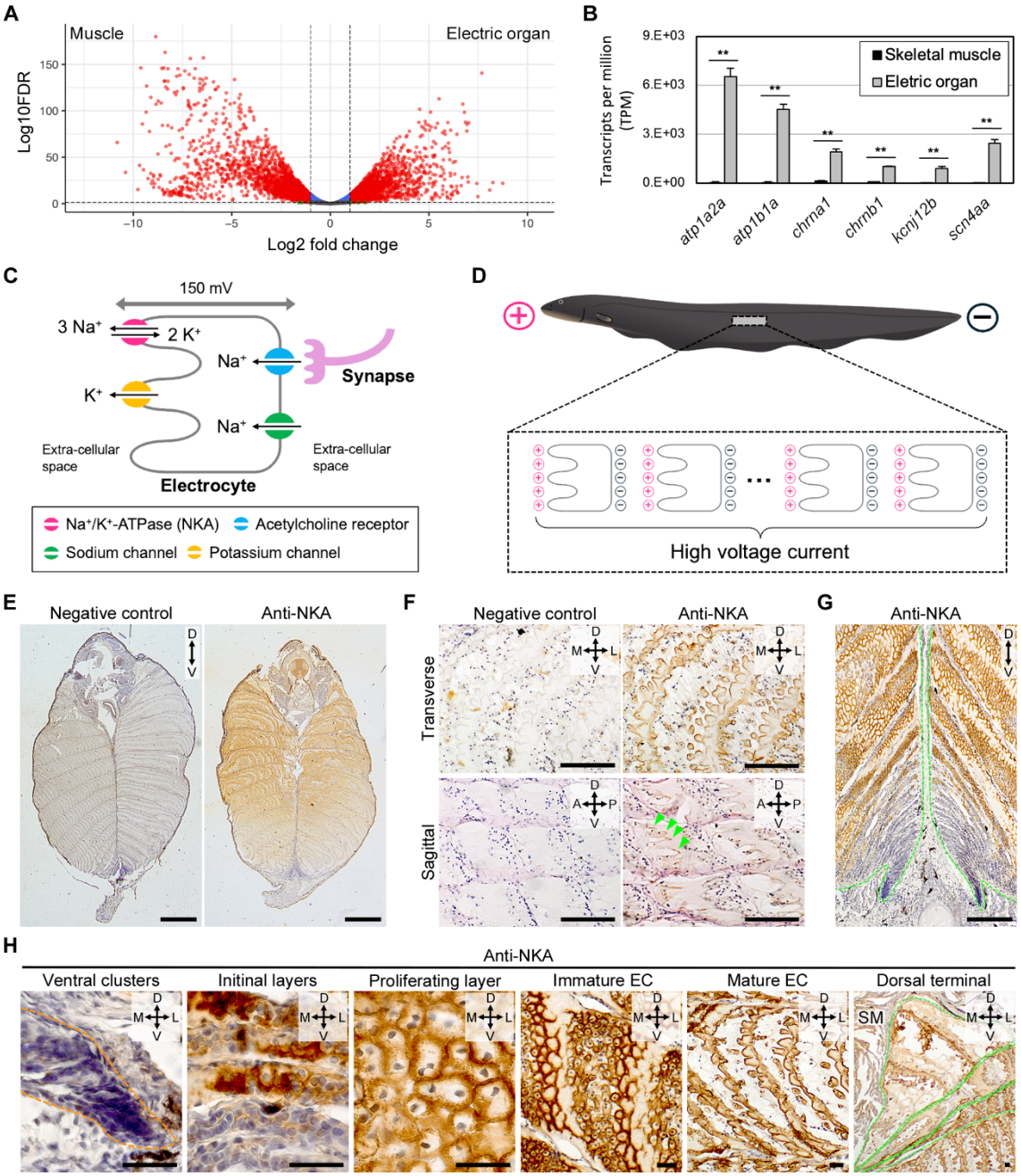

Figure 3. Presence and distribution of Na+/K+-ATPase in electric organ

A. Volcano map showing differentially expressed genes between skeletal muscle and mEO. Source data deposited in the DDBJ (ID: PRJDB17973). **B**. Comparison of gene expression values (TPM) for Na^+/K^+-ATPase (*atp1a2a*, *atp1b1a*), acetylcholine receptor (*chrna1*, *chrnb1*), potassium channel (*kcnj12b*), and sodium channel (*scn4aa*) between skeletal muscle and mEO. **C**. Schematic model illustrating the generation of membrane potential in an electrocyte, with ion transporters localized anteriorly or posteriorly on the cell surface, generating approximately 150

mV current due to synaptic input. **D**. Electrocytes arranged along the anterior–posterior axis, enhancing membrane potential leading to high-voltage discharge. **E**. Immunohistochemistry against NKA in transverse section. Scale bars, 1 mm. **F**. Enlarged images of anti-NKA immunohistochemistry in dorsal mEO in transverse and sagittal sections. Green arrowheads indicate anti-NKA signals on the anterior cell surface. Scale bars, 100 μm (transverse), 50 μm (sagittal). **G**. Ventral half of mEO in anti-NKA immunohistochemistry. Weaker anti-NKA signals observed in ventral terminal compared to dorsal regions. Scale bar, 100 μm. **H**. Enlarged images of anti-NKA immunohistochemistry in each cell type in the mEO. Orange dotted line indicates terminal ventral cluster. Green dotted lines indicate three layers from dorsal terminal of the mEO. Scale bar, 20 μm. A, anterior; D, dorsal; M, medial; L, lateral; P, posterior; V, ventral; SM, skeletal muscle.

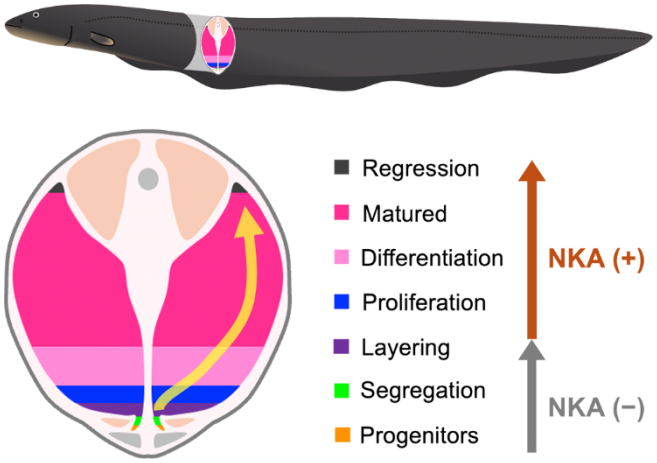

Figure 4. Model of main electric organ development

This illustration indicates the development of the main electric organ in the adult electric eel. Progenitor cells located in the ventral terminus of the main electric organ segregate and migrate dorsally, forming a layered structure. The NKA ion pump begins to be expressed at this stage. The cells in this layer proliferate and fuse into multinucleated syncytia. The syncytia differentiate into mature electrocytes and contribute to the generation of high-voltage discharges via ion transporters, including NKA. Electrocytes may regress to the dorsal terminus of the main electric organ.